

Structural Shape Optimization with Geometric Description and Adaptive Mesh Refinement

J. A. Bennett* and M. E. Botkin†

General Motors Research Laboratories, Warren, Michigan

Earlier work on shape optimization indicated that a simple problem description format was crucial to effective use of the program. As a result, a geometric problem description format which uses only boundary information was developed. A finite element mesh generation capability which requires only boundary information is used to generate the mesh, and a solution-based adaptive mesh refinement scheme is used to provide a more accurate estimate of the true solution. During the optimization process, periodic refinements are performed to generate estimates of the refined stresses based on unrefined solutions. Nonlinearities in the constraints led to some convergence difficulties; however, minimum mass designs typically were obtained in 30-40 finite element solutions.

Introduction

AN extensive amount of work has been done over the past two decades in the computer design of structural members. Most of this work has focused on a single aspect of this problem, such as finite element analysis, mesh generation, or structural optimization, rather than an integrated approach. Ultimately one would like merely to describe the function and limitations of the structure in some conceptually convenient terms and then allow the computer to automatically make adjustments in some way to produce a best design. The steps that are required in this process, whether or not they are automated, are as follows: model description; transformation of the model to an analysis description (finite element mesh); analysis (finite element analysis); analysis accuracy assessment; optimization; and convergence of the analysis-design sequence. While in the foreseeable future this process probably will not be automated for general structures, sufficient progress has been made to anticipate that it could be accomplished for simple components.

As has been described in previous work,^{1,3} the basic variables that one would usually want to change in the design process of a single component describe the shape of the part. Therefore, the process of transforming the design model to the analysis model cannot be done once but must be accomplished several times. This suggests that some type of automatic mesh generation⁴ will be required. The process of ensuring that the answers will be accurate could be addressed by mesh refining or updating techniques.⁵ Therefore, the steps outlined previously now become: model description; automatic mesh generation; analysis; mesh refinement and reanalysis; optimization; and convergence.

Since the topics of mesh generation and refinement are more developed for planar structures, this study will be limited to these structures. It should be noted, however, that many structures which are formed by bending or molding material into thin-walled, three-dimensional shapes could be considered as compositions of simpler two-dimensional subpieces. A newly constructed, integrated shape design computer program will be described herein. Each of the topics and their implementation in the program will be discussed. It should be emphasized that much of the effort here is to create a unified approach rather than to concentrate on perfecting one or more of the subtasks.

Model Description

The typical model description for structures for computer structural design has been the finite element model (geometry, connectivity, structural property information). This information is usually generated from drawings or sketches of the part. Thus, it is necessary to transmit information from a conceptual description of the part to an analysis description. In the design or optimization phase, changes in the conceptual or design description are made which affect the analysis or finite element description. For many problems which have been addressed by structural optimization, this difficulty has not been too significant because those design variables which have been permitted to change have described the structural property information (thicknesses, cross-sectional dimensions, etc.) and not the geometry or connectivity. In this case, it was convenient to think of a fixed finite element model with structural optimization data affecting only the property information. However, when considering a part such as the torque arm shown in Fig. 1, the design variables affect the geometry and connectivity also. In Ref. 1, the problem of generating the analysis model from the design description was handled by a design element concept in which the design variables were analytically linked to key nodes of large isoparametric elements (Fig. 2). The final mesh was generated using transformation methods in each of the large isoparametric design elements. Several drawbacks in this method became evident. A significant amount of time was required to build the design element model for each structure since the design element model is basically a finite element model. Further, any moderate changes in the design concept, such as changing from two to three holes, required completely rebuilding the design element model. Finally, the mapping

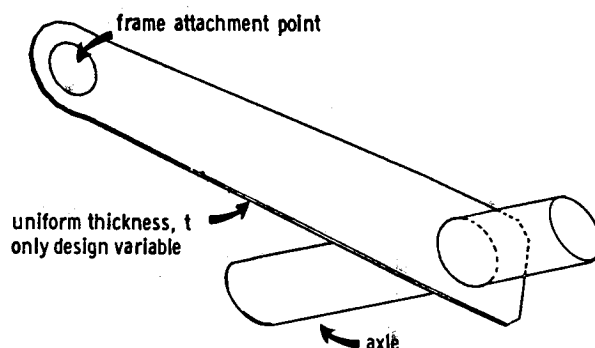


Fig. 1 Typical part.

Received Oct. 6, 1983. Copyright © American Institute of Aeronautics and Astronautics, Inc., 1984. All rights reserved.

*Assistant Head, Engineering Mechanics Department.

†Staff Research Engineer, Engineering Mechanics Department.

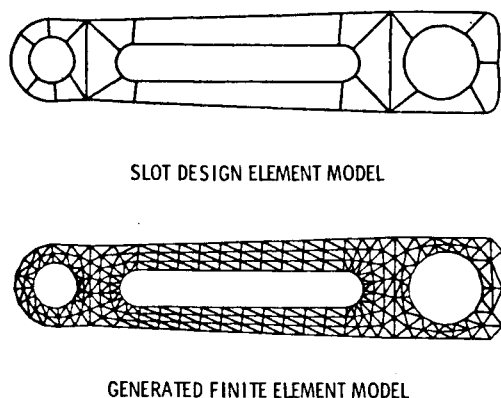


Fig. 2 Torque arm design element model.

type of mesh generation does not lend itself to automatic adaptive mesh generation. These considerations suggest that a more automatic approach to mesh generation be considered.

If one assumes the existence of an automatic mesh generation capability, the logical step is to consolidate, from the user's standpoint, the design and analysis models into a simple design model. This design model, however, is not to be considered static but rather as one that will be changed automatically throughout the design process, so it must retain information as to how the structure may vary.

A structure can be thought of as the material necessary to transfer a load from a point of application to a support point. Therefore, in its simplest form, a design model can be defined by its load and support points, lines, or surfaces. The load paths in the structure are the paths that connect these points. It seems logical that at some point only this basic information should be necessary to describe the part. On the other hand, the physical part itself is described by boundary lines in the case of two-dimensional parts and boundary surfaces in the case of solid parts. It would be possible to describe structures only in terms of some boundary information and connectivity; however, it was decided to try to retain some flavor of the load and support points and the load paths. Therefore, a series of both key nodes and boundary design elements has been developed. Each of the boundary elements is associated with key nodes which are located some distance from the ends of the boundary segment and would be load or support points (Fig. 3). Associated with each boundary element type is a set of design variables which will be changed by the optimization process. For instance, the key nodes in the torque arm shown in Fig. 4 would be the centers of the two attachment points. The closed boundary is then written as a sequence of boundary elements referenced to the key nodes. The direction of each boundary segment is determined by the lines connecting the referenced key nodes. For instance, in the triangular structure shown in Fig. 5, the first straight boundary segment runs from node 1 to node 2. The circular segment is rotated about node 2 where the angle is determined by the angles between lines 1-2 and 2-3. This pattern is continued until the boundary is closed. Loads and boundary conditions are associated with key nodes and boundary elements. In the torque arm, the loads could be applied to key node 1 and would be distributed automatically to the points on boundary 5 by a rigid finite element. Similarly, boundary 6 could be specified as fixed.

If one is restricted to thin-walled structures with large, relatively flat surfaces, this concept could be extended to three-dimensional structures with each relatively flat face being described in the previous fashion.

What has been created is a problem input format which describes the shape of the part in a form directly suitable for conceptual visualization, finite element mesh generation, and

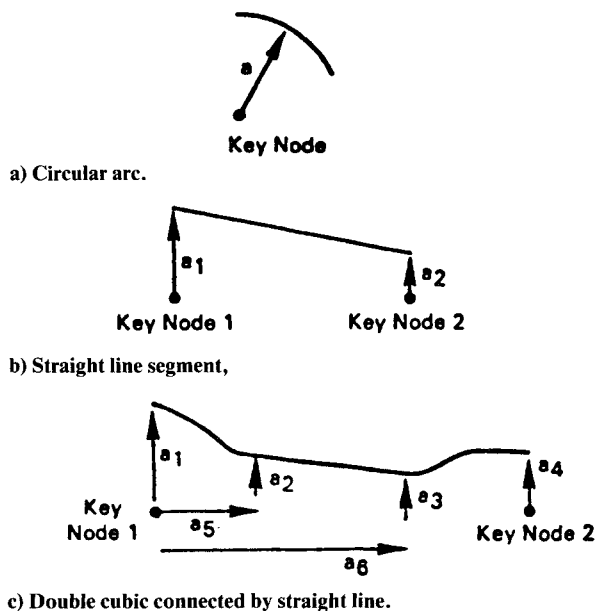


Fig. 3 Boundary design elements.

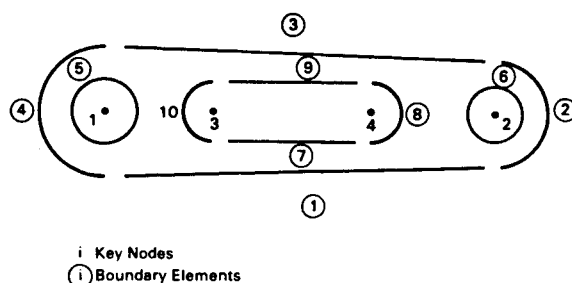


Fig. 4 Boundary elements for slotted torque arm.

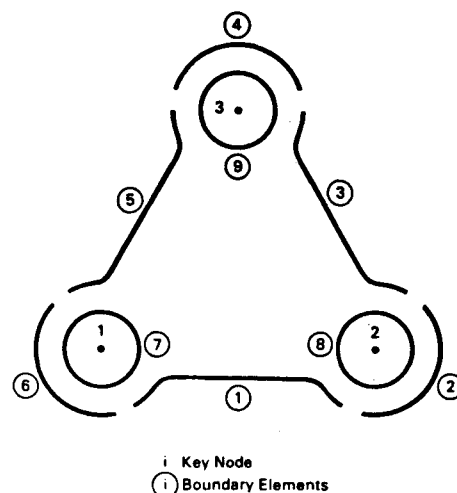


Fig. 5 Boundary elements for bracket.

optimization. This can be thought of as using geometric data as opposed to finite element data to define the problem.

Finite Element Analysis

Mesh Generation

In the previous section, it was assumed that techniques exist for automatically generating a finite element mesh for a two-

dimensional region given the boundaries of the region. The technique developed by Cavendish⁴ has been used to handle this task. This approach will divide a multiply connected closed region into triangular elements based on discretized description of the boundary. Thus, the boundary description format described in the previous section is quite appropriate. The sizes of the elements are determined by a characteristic length (CL) which must be selected for each problem. Automatic triangulation is used to create a set of connectivities for the discrete boundary points and points placed uniformly throughout the region's interior of approximately the same density as the boundary points (CL). The triangulation criterion is based upon an attempt to create equilateral triangles which is enhanced by the uniform spacing of the points. While it is generally accepted that constant strain triangular elements require more degrees of freedom to produce acceptable answers than quadrilateral elements, the ease of generating good triangular meshes from any boundary information outweighed this consideration. Questions of accuracy of the triangular meshes will be resolved through adaptive mesh refinement. Since this mesh generation technique is described in detail in Refs. 4 and 6, it will not be discussed herein. It should be noted that any dependence on interior region specification for mesh density, such as proposed in Ref. 4, is in conflict with the model description which is limited to boundary information only.

Mesh Refinement

When finite element analysis is used for a fixed configuration optimization, the integrity of the model is assured at the start of the optimization and assumed to remain acceptable throughout the design process. However, when the design process is changing the shape of the part and the shape and location of cutouts, this assumption is no longer valid. One way of handling this problem is to take advantage of the automated mesh refinement capabilities described in Ref. 5. In this concept, information from one analysis is used to identify regions of the finite element mesh which need further refinement. This refinement can take either the form of adding additional elements in the area to be refined or of increasing the order of the finite element. The mesh refinement approach has been chosen since it can be used with existing elements and does not require the formulation of new finite elements.

An example of the steps involved in the mesh refinement process can be seen in Fig. 6. The refinement criterion is based upon strain energy density (SED) variation within an element. A contour plot of the SED variation for the structure shown in Fig. 6a is shown in Fig. 6b. The elements contained within the dotted areas have undesirably high SED variations and will be refined by adding nodes as shown in Fig. 7. Each original element can have as many as three different subdivision patterns, depending upon the SED variation at the nearest node. The finest subdivision of Fig. 6b, i.e., the elements contained within the area covered by the smaller dots, would correspond to the pattern closest to node k of Fig. 7. Once nodes have been added to all of the required elements, the final mesh as shown in Fig. 6c was produced by retriangulating the resulting nodes.

As many as four levels of refinement, corresponding to the contours in Fig. 6b, may be chosen. The value of SED variation above which an element will be refined is obtained from the following expression⁶:

$$CV = \overline{\Delta E} + \beta (\Delta E_{\max} - \overline{\Delta E})$$

in which CV is the SED difference cutoff value, $\overline{\Delta E}$ the average SED variation for all elements, ΔE_{\max} the maximum SED variation in any element, and β a parameter to be selected based upon the problem but generally lies between 0 and 0.5.

As applied in the literature, adaptive finite element analysis is thought of as a static process; that is, the model for the

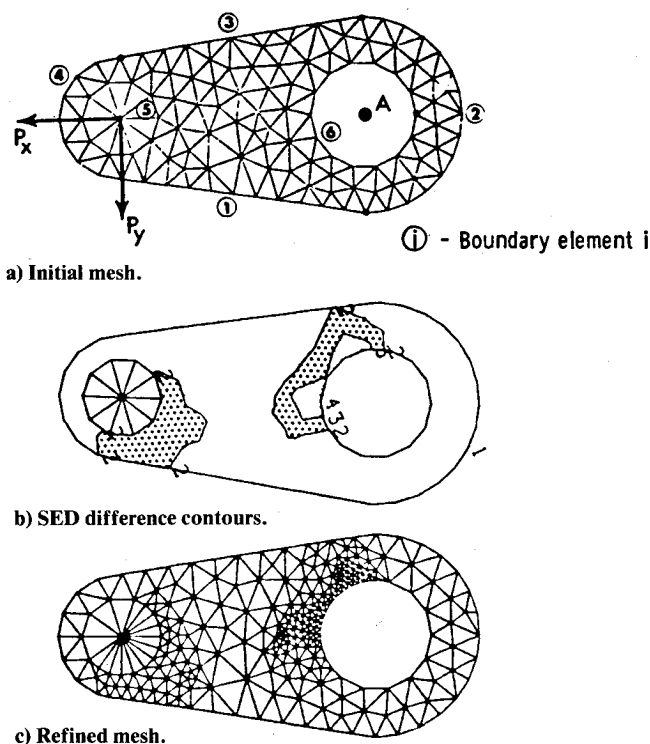


Fig. 6 Multi level refinement.

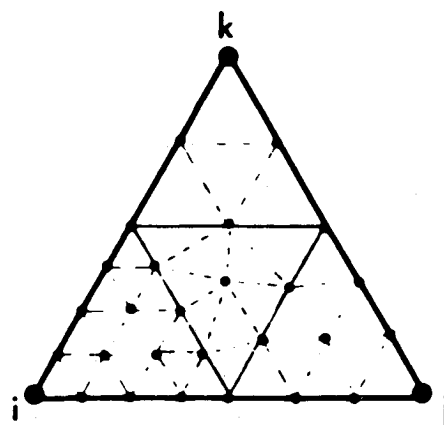


Fig. 7 Element refinement pattern.

existing design is altered until either the answers converge or some error tolerance is achieved. In general, this process will require more than one finite element solution. In optimization, it will be necessary to consider a more dynamic process since the design will be changing continually, and it will be necessary to predict the behavior of the constraints as the design changes. Since the optimization process requires many analyses by itself, it is reasonable to search for ways to reduce the number of refinements required during the optimization process.

The results of several analyses of the part shown in Fig. 8 are shown in Fig. 9 for two types of constraints. One constraint is at the narrow end of the slot and the other is on the outside near the root. In these figures, the stress is plotted as a function of the square root of the area (\sqrt{A}) of the element which is a measure of the element size. Each constraint is evaluated with two unrefined meshes (characteristic lengths of 1.0 and 0.75) and four refined meshes. What is required is the correct value of the stress which, for a convergent element, would be obtained as the element size is reduced to zero. It was proposed in Ref. 6 that this value could be approximated by a linear extrapolation based on unrefined and refined analyses.

As Fig. 9 shows, this approximation is not unreasonable and, in general, will tend to overestimate the stress in an infinitely small element. As was pointed out in Ref. 6, this may not be true for bending elements. It does not appear that the increased computational effort required to compute a second-order approximation would be warranted.

The approach to be used, therefore, is to perform coarse and refined analyses and to use this information to construct a linear approximation to the actual stresses based on the coarse analysis. This approximation will then be used until some later time when a new refined analysis and an updated approximation will be generated. The actual application will be described in the discussion of the optimization methods used.

Optimization Techniques

The same considerations that affect traditional structural optimization will be important in shape optimization; that is, the number of analyses should be small and the derivatives should be calculated as efficiently as possible. In this paper, the derivative computations will not be addressed, and it will be assumed that they are available. In the later examples, both finite difference and implicit differentiation formulas [$\partial u / \partial x = -K^{-1} (\partial K / \partial x) \{u\}$] have been used.

Treatment of Stress Constraints

There are inherent difficulties associated with treating stress constraints in discretized structures which are compounded when shape is used as a design variable. If the stress data point is a continuous function of the design variables, the finite element stress results can only approximate this function which results in a highly nonlinear constraint behavior characterized by many local peaks and valleys. To some extent, this nonlinearity is inevitable as the remeshing guarantees some of this behavior.

In addition, some decision must be made as to how the constraints are to be defined. Associating the constraints with a finite element is unattractive since the finite element mesh will change during the design process. Clearly the stress constraint needs to be associated with some point in the structure. For the present time, the following limited approach has been chosen. It is assumed that the maximum stress occurs along a boundary; therefore, the stress constraints will be associated with each boundary element. For this purpose each boundary element can be broken into a predetermined number of stress constraint segments. In each segment, the stress constraint is taken as the maximum stress in any finite element touching that segment of the boundary.

Method of Optimization

The traditional methods of nonlinear optimization have two severe drawbacks for extensive shape optimization. First, they permit large excursions in the design variables which may be not justified based on the starting finite element analysis. This radically altered design may be so infeasible as to seriously compromise the convergence of the optimization. Second, they tend to spend most of the computational time tracking active constraints. The irregularity of the constraints will seriously compromise this convergence process. In addition, of course, the direct methods require an excessive number of finite element solutions.

The approximation concepts,⁷ on the other hand, seem to be more suited to this type of problem. Since they impose intermediate move limits on the design variables, large changes in the shape can be limited. This also allows for an orderly introduction and updating of the extrapolation for the constraint values based on coarse mesh solutions as described earlier. The idea that is being proposed is deficient in that, as the mass is reduced, the approximation used to predict the stress level becomes more unconservative. Therefore, at the end of each step, the design is usually infeasible and, in general, more infeasible than the approximations predict. The

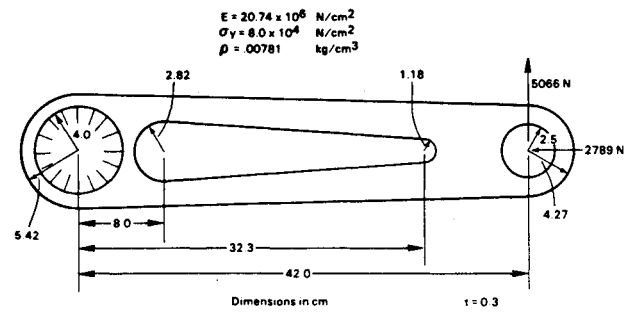


Fig. 8 Torque arm dimensions for convergence tests.

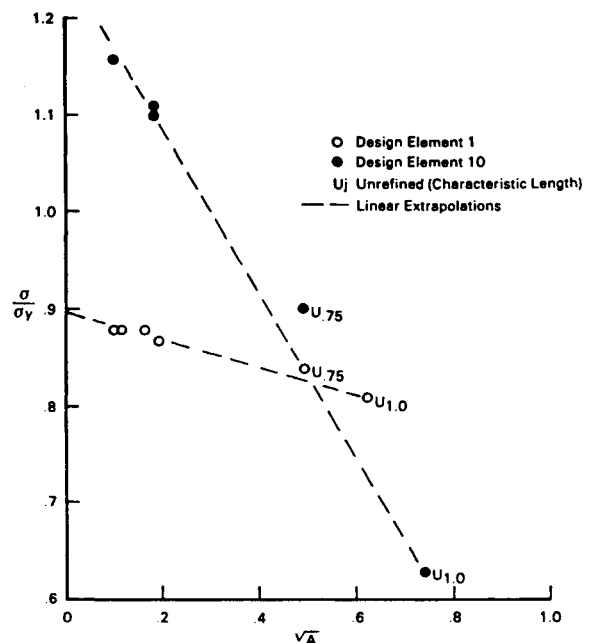


Fig. 9 Convergence of stress constraints.

feasible directions program, CONMIN, was used to solve the approximate problem.

When the approximation concepts are used, the success of the optimization is often determined by the side constraints imposed on the approximate problem, which are usually called move limits. The particular implementation of move limits used is based on a percentage of the total motion allowed. Then, for the j th subproblem,

$$x_{i,upper,lower_j} = (x_i)_{j-1} \pm \Delta (x_{i,upper_0} - x_{i,lower_0})$$

$i = 1, 2, \dots$, number design variables

where the subscript 0 refers to the original, nonsubproblem upper and lower bounds and Δ is a global move parameter that refers to all design variables. In this formulation, the amount of motion is not dependent on the current value of the design variable. This is important because some design variables such as a_2 and a_3 of the double cubic (Fig. 3) may pass through zero, and a move limit given as a percentage of the current value would produce very slow motion around zero.

Stress Approximation

As described earlier, an extrapolation scheme will be used to approximate the actual stresses from an unrefined analysis based on a previously refined analysis. This will be handled by

the following relationship:

$$\sigma_a^e = \sigma_c^e + \lambda A_c^{1/2}$$

where σ_a^e is the approximate value of the actual maximum element stress, σ_c^e the maximum element stress for the coarse mesh, A_c the coarse element area, λ the stress approximation parameter, and

$$\lambda = \frac{(\sigma_f^e)_n - (\sigma_c^e)_n}{(A_f)^{1/2}_n - (A_c)^{1/2}_n}$$

where subscripts f and c refer to fine and coarse meshes and n indicates that λ is updated at step n .

Table 1 λ histories

Step No.	Example 1 small end of slot (BE ₁₀)	Example 2 top of hole (BE ₁₃)
0	-0.50	-0.50
5	-0.66	-0.50
10	-0.75	-0.50
15	-0.59	-0.50
20	-0.50	-0.50
25	-0.53	-0.50
30	-0.50	-0.71
35	-0.50	-0.93
40	-0.50	
45	-0.50	

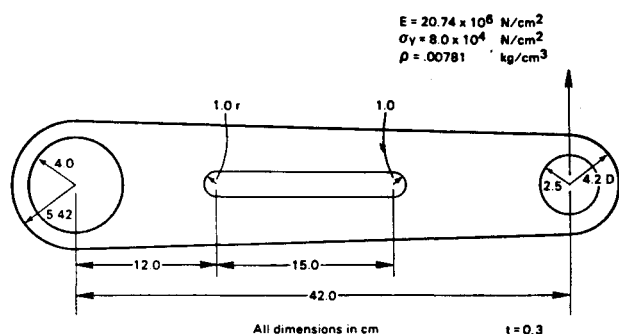


Fig. 10 Structure for example 1.

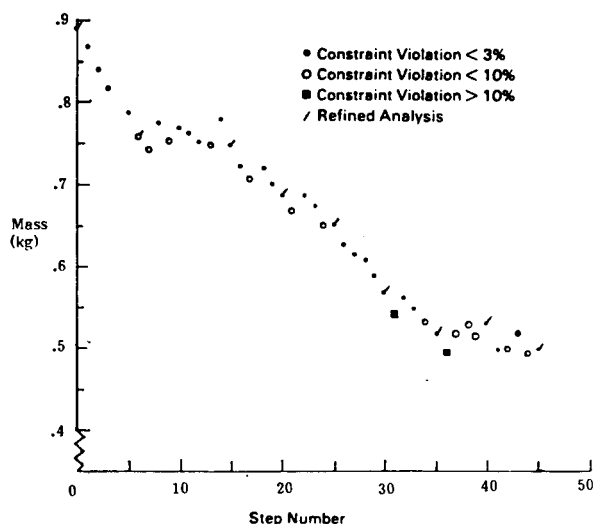


Fig. 11 Iteration history example 1.

Clearly, if significant changes in the design are experienced before λ is updated, the updated design will be significantly infeasible and instabilities in the design algorithm will result. One approach is to update frequently, which, to some extent, defeats the purpose of using this approximation. Another alternative is to select an arbitrary value of λ , say λ_0 , to be used at all times when λ is calculated to be smaller than λ_0 . If this λ_0 is judiciously chosen, it tends to protect against excessive reduction in material leading to the previously mentioned instability. For the examples discussed later, $\lambda_0 = -0.5$ with updates every five steps has proven satisfactory.

Geometric Behavior Constraints

An aspect of shape optimization that has caused difficulty in the past is how to keep boundaries from intersecting as the design changes. Many times, typical behavior constraints such as stress or displacement will not control boundary movement sufficiently, resulting in the boundaries intersecting each other. The way this has been handled in the past is to put side constraints on the dimensions. This, of course, works well as long as the boundaries are a function of a single dimension only. For instance, in the torque arm of Fig. 8, if the centers of the inside radii were not variables, then side constraints on

Table 2 Final design variables

Example 1 (mass = 0.5 kg)		Example 2 (mass = 0.135 kg)	
n_{1x}	10.18	n_{1x}	6.81
n_{2x}	33.42	n_{1y}	1.57
		n_{2x}	13.07
BE ₁		n_{3y}	10.49
a_2	1.89		
a_3	4.59	BE ₁	
a_5	10.16	a_2	-0.04
a_6	29.07	a_3	-0.04
		a_5	2.5 _s
BE ₈		a_6	7.5 _s
a	0.65 _s		
		BE ₃	
BE ₁₀		a_2	1.22
a	3.20	a_3	0.91
		a_5	2.62
		a_6	12.41

Note: n_i = node i ; BE _{i} = boundary element i ; s = at side constraint.

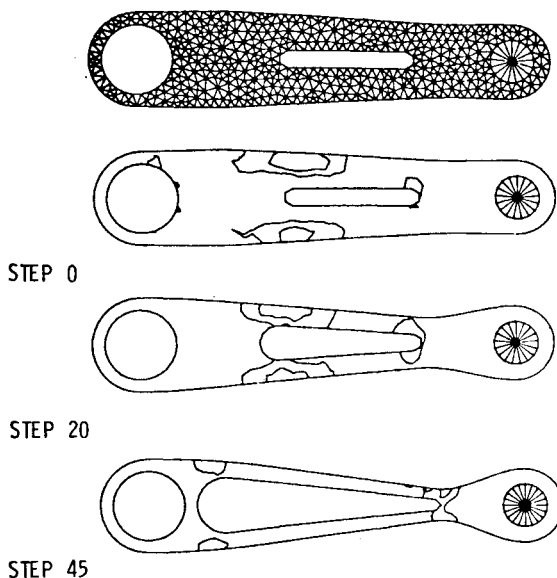


Fig. 12 Shape history example 1.

these radii would maintain precise control over possible boundary intersections. However, once the centers are allowed to move, each variable must be limited by the worst-case combination. For example, for the slot in Fig. 8, an upper limit must be placed upon the radius and then a limiting value assigned to the x coordinate of the key node. But, if the radius never reaches its upper limit, then the holes will be kept apart by the limit on the x coordinate when they actually should not be. This problem could be handled by a higher level side constraint, such as side constraint linking, but this may not even work for more complicated, polynomial-based boundary shapes.

The solution to the problem is to define a new kind of behavior constraint referred to as the geometric behavior constraint and defined to be the distance between boundary segments. A constraint is assigned for each boundary segment in combination with every other segment, except for those segments which are on a common closed boundary curve. The relationship for computation of the number of constraints is

$$ngc = \frac{1}{2}[(n-1)n - \sum_k (m_k - 1)m_k]$$

in which n is the total number of boundary design elements, k the number of closed boundaries which are composed of more than one boundary design element, and m_k the number of boundary elements on boundary k .

The constraint values are calculated by a double loop through the coordinates of all boundary points, which have been stored continuously at the beginning of the list, computing the minimum distance between each point and every other point, and then retaining only the minimum value for each boundary segment. The distance computation is further refined by computing the actual distance between tangents to the discrete segments.

Example Problems

Two example problems will be shown to demonstrate shape optimization with automatic mesh refinement. Both examples were stress constrained.

Example 1

This structure is shown in Fig. 10. Design element 3, the double cubic, was used to describe the long outside boundaries of the structure with four design variables associated with each side of the boundary. In addition, the longitudinal location of the slot ends and the radii of the slot ends were allowed to vary for a total of eight shape design variables. λ_0 was chosen to be -0.5 . Minimum boundary separation was 1.0. An iteration history is shown in Fig. 11, the λ history in Table 1, the design variable history for key boundary elements in Table 2, and the boundary shape of the part in Fig. 12. In the iteration history, three levels of constraint satisfaction are shown. Small dots represent less than 3% violation and will be considered feasible. Open circles (greater than 5% but less than 10% violation) and solid squares (greater than 10% violation) will be considered infeasible. In the boundary shape history, the SED gradient contour will be shown, rather than the refined meshes, for clarity. The characteristic length (CL) was 0.9 and the move limit (Δ) was 0.025.

Initially, there is no difficulty associated with the stress concentrations around the slot; however, at step 5 the refinement increased the approximation parameter to -0.66 . It was not until step 20 that this difficulty was resolved and the basic taper shape started to evolve. The remaining steps were used to reach the final shape. In these last steps many of the unrefined analyses were infeasible, while the refined analyses are feasible. Two effects contributed to this behavior. The 0.9 characteristic mesh produces a rather coarse mesh which leads to both difficulties in precisely predicting the stresses from the Taylor series expansion and in noise in the stress prediction due to remeshing. However, if

the choice of λ_0 is conservative (i.e., the stresses converge faster than λ_0 predicts), the stresses from the unrefined meshes will be larger than those finally predicted from the refined mesh since the extrapolation is always based on the most refined mesh available.

This suggests that several other strategies might be used in the final stages of the design to improve convergence. The characteristic length was reduced to 0.75 which produced more accurate expressions for the stresses and allowed a slightly lower mass. Reducing the step size did not markedly affect these results. Reducing λ_0 to -0.33 allowed a reduction in the mass (0.09 kg) with considerable instability in the feasibility of the designs. The reduced λ_0 runs were generally quite erratic and produced many infeasible designs. This latter portion of the design is attempting to hold the stress constraint at the small end of the slot while enlarging both the outside boundary and the large end of the slot. This involves a fairly complex relationship between the design variables, the

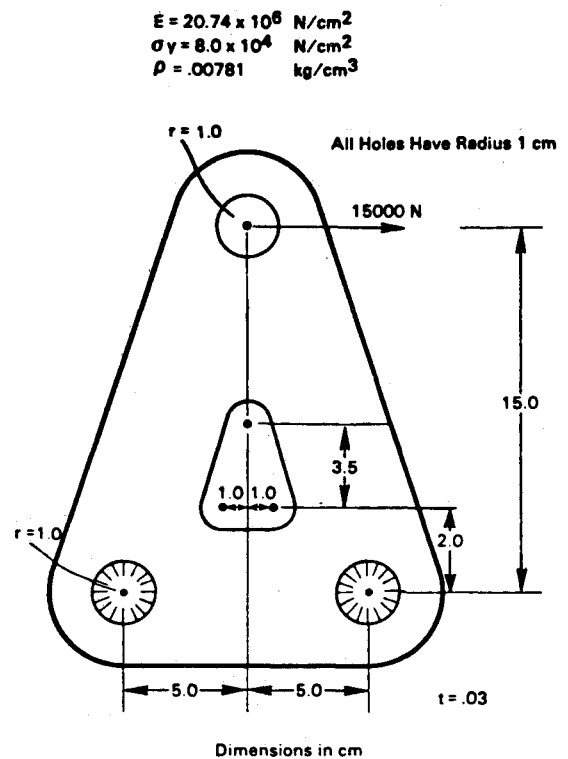


Fig. 13 Structure for example 2.

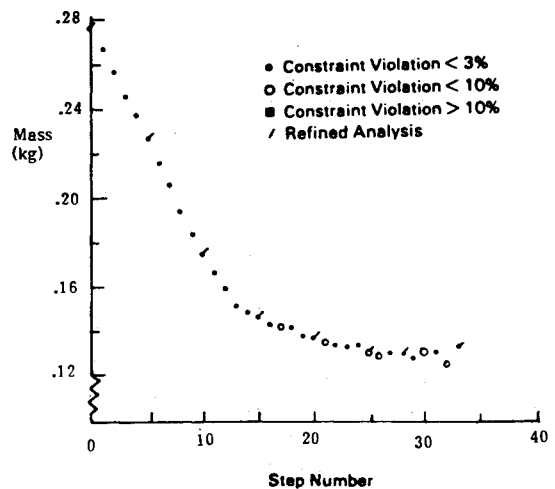


Fig. 14 Iteration history example 2.

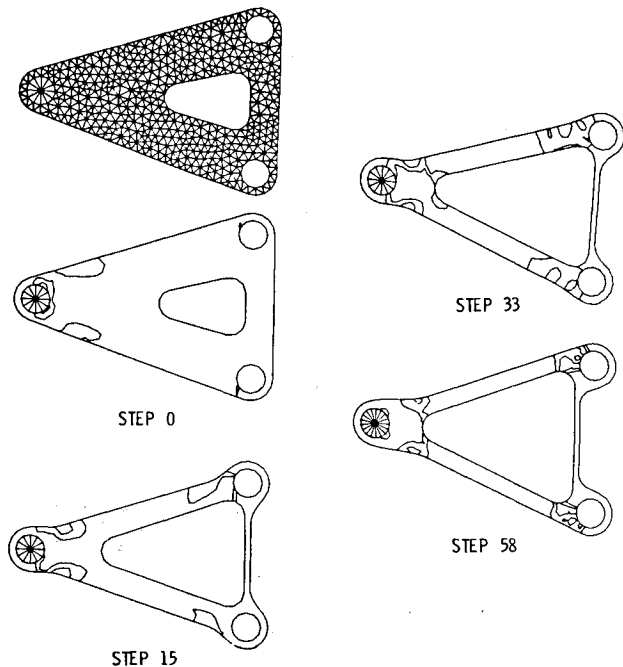


Fig. 15 Boundary shapes and refinement areas for example 2.

stress constraints, and the geometric constraint between the large end of the slot and the mounting hole which appears to be quite difficult to follow.

Example 2

The initial shape of the bracket is shown in Fig. 13. For this problem, all three outer edges were of the double cubic format with four design variables on each edge. The center of each corner radius of the hole was allowed to vary with the top of the hole constrained to be on the centerline. The two slanted sides were linked in such a way that a symmetric design was produced; a total of 11 boundary design variables was used. The slanted sides were split into three stress constraint regions each. λ_0 was again chosen to be -0.5 ; the minimum boundary separation was 0.36 . The initial characteristic length was 0.5 and the move limit was 0.025 . The iteration history is shown in Fig. 14, the λ history in Table 1, the design variables for key boundary elements in Table 2, and the boundary history of the part in Fig. 15.

The initial steps of this example are quite smooth since, unlike the first example, the initial shape of the hole was quite similar to the final hole shape. Some difficulty was encountered after step 15 in tracking the stress constraint around the top of the hole. This was resolved by modifying the upper and lower bounds on this design variable so that the effective move limit was reduced although the global move limit remained the same. This run terminated with a feasible design at step 28. At this point, the characteristic length was changed to 0.35 and run for five additional steps. This indicates that the result obtained with the coarser (0.5) mesh was adequate to obtain satisfactory answers. The λ history as shown in Fig. 14 indicates that λ_0 was not a conservative estimate at the final design, but the λ values appear to be converging. This design was allowed to continue for several additional steps. There is a fairly small change in the mass between step 33 and 58 (0.02 kg or 14%) relative to the effort required to achieve it. As can be seen from the boundary history, this is accomplished by moving the bottom "bar" up,

allowing the hole to move further out. This behavior of a rather slow convergence was observed in the first example also.

Conclusions

An integrated approach to the shape design problem in which the problem description is stated in a simple format, the finite element mesh is generated automatically, and its accuracy is improved by adaptive mesh refinement is described here. Since a boundary description of the part is used and the mesh is generated automatically, the technique is not limited to relatively small changes from an initial design. In fact, any design which is permitted by the initial boundary topology is realizable. This behavior has been adequately demonstrated by the examples.

While much work has been done with mesh generation in the past, most of it has ultimately relied on either a complex input format or user interaction to read just bad meshes. In the present situation, a very robust mesh generator is required in that a slightly inaccurate mesh is preferable to an incomplete mesh. At the time this work was begun, triangular mesh generations were clearly more reliable and less dependent on complex information or user interaction. While it is clearly understood that triangular meshes may be less efficient or less accurate, the combination of robust mesh generation and adaptive mesh refinement makes this approach quite attractive.

From the problems attempted with this technique, several factors have emerged. Because the mesh is regenerated for each analysis, the displacement and stress results during the design process will be noisy and introduce a degree of difficulty that typically has not existed in most structural optimization problems. The approach used of a sequence of approximate problems is one way to handle this difficulty since, in each approximate problem, the Taylor series approximations will produce continuous stresses and displacements. Second, it is desirable not to require a complete adaptive solution each time an analysis is required. Some method of approximating the true solution from a less accurate solution is desirable. The linear extrapolation scheme based on the most recent refined solution that was proposed here is quite simple and does not appear to lead to instabilities.

References

- Botkin, M. E., "Shape Optimization of Plate and Shell Structures," *AIAA Journal*, Vol. 20, Feb. 1982, pp. 268-273.
- Imam, M. H., "Three-Dimensional Shape Optimization," *International Journal for Numerical Methods in Engineering*, Vol. 18, No. 5, 1982, pp. 635-673.
- Imam, M. H., "Minimum Weight Design of 3-D Solid Components," *Proceedings of the Second International Computer Engineering Conference*, ASME, Vol. 3, San Diego, Calif., Aug. 1982, pp. 119-126.
- Cavendish, J. C., "Automatic Triangulation of Arbitrary Planar Domains for the Finite Element Method," *International Journal for Numerical Methods in Engineering*, Vol. 8, No. 4, 1974, pp. 679-696.
- Shephard, M. S., Gallagher, R. H., Abel, J. F., "The Synthesis of Near-Optimum Finite Element Meshes with Interactive Computer Graphics," *International Journal for Numerical Methods in Engineering*, Vol. 15, No. 7, 1980, pp. 1021-1039.
- Botkin, M. E., "An Adaptive Finite Element Technique for Plate Structures," *Proceedings of the AIAA Structures, Structural Dynamics and Materials Conference*, Lake Tahoe, Nev., May 1983, Paper 83-1009.
- Schmit, L. A., Miura, H., "A New Structural Analysis/Synthesis Capability—ACCESS 1," *AIAA Journal*, Vol. 14, May 1976, pp. 661-671.